

The Lipid-binding Domain of Wild Type and Mutant α -Synuclein

COMPACTNESS AND INTERCONVERSION BETWEEN THE BROKEN AND EXTENDED HELIX FORMS^{*§}

Received for publication, December 15, 2009, and in revised form June 24, 2010 Published, JBC Papers in Press, June 30, 2010, DOI 10.1074/jbc.M110.157214

Elka R. Georgieva[‡], Trudy F. Ramlall[§], Peter P. Borbat[‡], Jack H. Freed^{‡1}, and David Eliezer^{§2}

From the [‡]Department of Chemistry and Chemical Biology, Cornell University, Ithaca, New York 14853 and the [§]Department of Biochemistry and Program in Structural Biology, Weill Cornell Medical College, New York, New York 10065

α -Synuclein (α S) is linked to Parkinson disease through its deposition in an amyloid fibril form within Lewy Body deposits, and by the existence of three α S point mutations that lead to early onset autosomal dominant Parkinsonism. The normal function of α S is thought to be linked to the ability of the protein to bind to the surface of synaptic vesicles. Upon binding to vesicles, α S undergoes a structural reorganization from a dynamic and disordered ensemble to a conformation consisting of a long extended helix. In the presence of small spheroidal detergent micelles, however, this extended helix conformation can convert into a broken helix state, in which a region near the middle of the helix unwinds to form a linker between the two resulting separated helices. Membrane-bound conformations of α S likely mediate the function of the protein, but may also play a role in the aggregation and toxicity of the protein. Here we have undertaken a study of the effects of the three known PD-linked mutations on the detergent- and membrane-bound conformations of α S, as well as factors that govern the transition of the protein between the extended helix and broken helix states. Using pulsed dipolar ESR measurements of distances up to 8.7 nm, we show that all three PD-linked α S mutants retain the ability to transition from the broken helix to the extended helix conformation. In addition, we find that the ratio of protein to detergent, rather than just the absolute detergent concentration, determines whether the protein adopts the broken or extended helix conformation.

Since its initial discovery as a protein enriched in the electric organ of the Pacific electric ray, *Torpedo californica* (1), the protein α -synuclein has been progressively associated with a role in neurodegeneration in humans, starting with its identification as the precursor protein of a non-amyloid- β peptide component of amyloid plaques (the so-called NAC peptide) (2) and culminating in its discovery as the first gene product to be linked to familial Parkinson disease (3) and its contemporane-

ous identification as the primary component of the fibrillary aggregates found in the hallmark Lewy body deposits associated with Parkinson (4).

Subsequently, a great deal of effort has been made to clarify and understand the mechanisms by which α S causes neuronal degeneration, as well as to understand the normal functional roles of α S and how these are related to its role in disease (5, 6). Although aggregation of α S remains a key focus in these efforts, it remains possible that other, or additional, effects beyond the presence of various aggregated species of α S may be involved in the etiology of synuclein-associated PD. A key piece of the puzzle that remains unanswered is which of the various forms of α S that have been observed *in vitro* are involved in mediating the toxicity of the protein *in vivo*. In particular, although α S is highly disordered when isolated in solution *in vitro* (7–9) it is not clear to what extent this intrinsically disordered state is populated *in vivo*. Because α S has been shown to interact with lipid membranes and synaptic vesicles *in situ* (10–13) membrane-bound forms of the protein are likely to be populated in living cells. Thus, membrane-bound conformations of the protein may provide clues regarding both the normal and pathological pathways in which α S participates.

Early spectroscopic studies of membrane-bound α S revealed a highly helical structure (14–16). More detailed studies using membrane-mimetic spheroidal detergent micelles showed that this structure could take the form of two individual helices, separated by a non-helical linker (17, 18) and aligned anti-parallel to each other on the micelle surface (19). Subsequent ESR studies confirmed this broken helix structure by explicitly measuring distances between the two helices (20). More recent ESR work also demonstrated that when α S is bound to lipid vesicles, lipid bicelles, or rod-like detergent micelles, the protein can take the form of a single extended helix, based on direct measurement of the ensuing long (4–7.5 nm) distances (21) and also on modeling using shorter (2–4 nm) measured distances (22). This result was further confirmed by recent fluorescence-based measurements (23, 24). In addition, it was observed that the protein can apparently interchange between the broken helix and extended helix conformations (21, 23).

Here we have undertaken studies of the effects of PD-linked mutations on the membrane- and detergent-bound conformations of α S, as well as of the factors that govern the interconversion of the protein between the broken helix and extended helix conformations. We find evidence that α S fluctuates

* This work was supported, in whole or in part, by National Institutes of Health Grants AG019391 and AG025440 (to D. E.) from the NIA and NCRR P41-RR016242 and NIBIB EB03150 (to J. H. F.), the Irma T. Hirsch Foundation, and a gift from Herbert and Ann Siegel (to D. E.).

§ The on-line version of this article (available at <http://www.jbc.org>) contains supplemental Figs. S1–S3 and Tables S1 and S2.

¹ To whom correspondence may be addressed. E-mail: jhf3@cornell.edu.

² To whom correspondence may be addressed. E-mail: dae2005@med.cornell.edu.

Helix Interconversion of α -Synuclein

between compact and extended conformations when the protein is free in solution, in the absence of membrane or detergent. We also confirm previous reports that in the presence of detergent, the conformation selected by α S is dependent on the detergent concentration (23, 25). Interestingly, however, the detergent concentration alone does not always dictate whether the extended or broken helix structure will form. Instead, the protein-to-detergent ratio is also a determinant of which structure is observed. This suggests that whereas the membrane environment exerts an influence on the conformation of the protein, the protein in turn can affect the membrane structure. Finally, we find that the PD-linked α S mutations remain capable of adopting both the broken helix and extended helix forms of the protein. The implications of these observations are discussed.

EXPERIMENTAL PROCEDURES

Protein Expression and Purification

Double cysteine mutants of wild type (WT), and Parkinson disease (PD)³ mutants A30P, E46K, and A53T of α S were expressed, purified, and spin-labeled with MTSSL as described in the literature (8, 20, 26, 27). A subset of residues used by us in previous studies of the WT protein (20, 21) was selected for mutation to cysteine, including Gln-24, His-50, Glu-61, Thr-72, and Glu-83.

Preparation of Micelles, Bicelles, and Liposomes

1,2-Dimyristoyl-*sn*-glycero-3-phospho-(1'-rac-glycerol), sodium salt (DMPG and DMPG-d54), 1,2-dimyristoyl-*sn*-glycero-3-phosphocholine (DMPC and DMPC-d67), and 1,2-dihexanoyl-*sn*-glycero-3-phosphocholine (DHPC) were purchased from Avanti Polar Lipids. Fully deuterated SDS-d25 was purchased from Sigma. All compounds were used as received. Five different membrane mimetics were used: 1) spheroidal micelles at low concentration of SDS-d25 (from 5 to 60 mM); 2) lyso-1-palmitoyl-phosphatidylglycerol (LPPG) micelles with LPPG concentration of 40 and 80 mM; 3) rod-like micelles prepared at 450 mM SDS-d25; 4) DMPC/DMPG/DHPC bicelles with q (the ratio of long chain to short chain lipids) of 2.6 and [DMPC] to [DMPG] ratio of 8.75; and 5) liposomes composed of DMPC/DMPG in a 1:1 molar ratio. The LPPG micelles, rod-like SDS micelles, bicelles, and liposomes were prepared as described previously (20, 21).

Distance Measurements by DEER Spectroscopy

All measurements have been performed at 17.3 GHz and 60 K using a home-built Ku-band pulse FT-ESR/DQC spectrometer (28–30) set to operate in 4-pulse DEER mode (21, 31). The $\pi/2$ and π pulses of the detection mode had widths of 16 and 32 ns. The pump pulse typically was set to 32 ns, but was 20 ns in some cases. The pump pulse was set at the central maximum of the nitroxide spectrum. The detection frequency was 70 MHz

above the pumping frequency, corresponding to the low-field edge of the nitroxide spectrum. The spin-spin distances in some of the double mutants, in particular 24/83, were as large as 8.7 nm, necessitating the use of evolution times as long as 14 μ s. For such long evolution times the spin echo amplitude decays by phase relaxation, leaving no detectable signal in spin-labeled proteins. To overcome this challenge, we used 70% deuterated proteins with spin labels at positions 24 and 72, and 24 and 83. In addition, DMPC-d67 and DMPG-d54 were used for liposome or bicelle preparations. By these means the phase relaxation was sufficiently suppressed, enabling evolution times as long as 14 μ s (see [supplemental materials](#)). In cases of shorter distances, depending on the particular sample the signal averaging time varied from 2 to 10 h. The time domain signals for proteins, having spin labels at positions 24 and 72, and 24 and 83, were averaged over periods of nearly 30 h. The pulse repetition rate was 1 kHz in all measurements.

Protein and Spin Concentrations

Protein stock solutions were prepared by dissolving lyophilized protein in the appropriate buffer and concentrations were determined based on the mass and volume used. Samples for measurement were prepared through dilutions using the stock solutions. To assess the degree of spin labeling, we used a standard sample of 100 μ M 4-hydroxy-TEMPO-free radical in D₂O: Gly-d8 as a reference to estimate the spin concentration per total protein concentration, by quantitative comparison of initial spin-echo intensities. Spin labeling efficiency was estimated, and was typically found to be less than 100%. In particular we estimated relatively low spin labeling efficiency at positions 72 and 83. Importantly, the presence of unlabeled protein would not affect any of the results or conclusions presented here, which are based on total protein concentration.

Data Analysis

The distance analysis of experimental time domain data has been conducted using the L-curve Tikhonov regularization method (32) to yield inter-spin distance distributions from which average distances and their variations were inferred. The distance distributions produced by the L-curve method were refined, as needed, by the maximum entropy method (MEM) (33). In some cases, to aid in the interpretation of these distance distributions we further analyzed them by fitting them with one or two Gaussians, using a MATLAB script developed in our laboratories (see [supplemental data](#)). In all cases the distance distributions (or their Gaussian representations) were characterized in terms of average distance, R , and their full width at half-maximum, abbreviated as ΔR . Distance distributions from more than 100 sets of data were obtained in this study.

Sample Preparation for DEER Measurements

Proteins in Free State—WT α S and its PD-liked mutants with spin labels at positions 24/61, 24/72, and 24/83 were prepared in 1:1 D₂O:glycerol-d8, pD 7.4. The protein concentration was 100 μ M.

Membrane-bound Proteins—WT α S and its PD-liked mutants with spin labels at positions 50/72, 24/61, 24/72, and 24/83 were prepared in solutions of spheroidal SDS or LPPG

³ The abbreviations used are: PD, Parkinson disease; DMPG, 1,2-dimyristoyl-*sn*-glycero-3-phospho-(1'-rac-glycerol), sodium salt; DMPC, 1,2-dimyristoyl-*sn*-glycero-3-phosphocholine; DHPC, 1,2-dihexanoyl-*sn*-glycero-3-phosphocholine; LPPG, lyso-1-palmitoyl-phosphatidylglycerol; MEM, maximum entropy method.

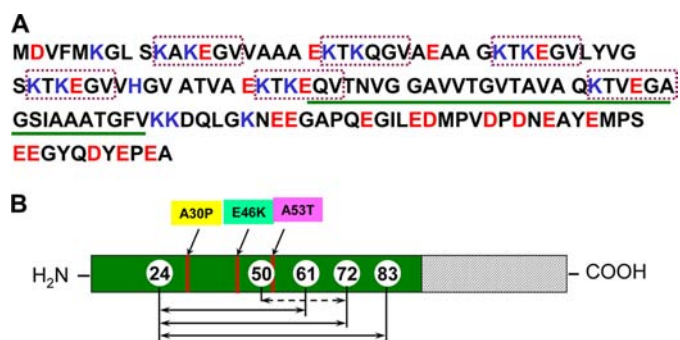


FIGURE 1. *A*, amino acid sequence of WT α S. The basic amino acids are colored blue; the acidic amino acids are colored red; the six imperfect repeats of 11 amino acids with the conserved core KTKEGV are in dotted rectangles in magenta; the green bar shows the non-amyloid component (NAC), residues 61–95. *B*, schematic representation of α S polypeptide chain. The N-terminal and NAC domains are colored green; the C-terminal domain gray. The positions of three point mutation A30P, E46K, and A53T are shown. The numbers in white circles show the spin-labeled residues and the connecting arrows show the measured inter-spin distances, respectively.

micelles, rod-like SDS micelles, DMPC/DMPG liposomes, and DMPC/DMPG/DHPC isotropic bicelles. The protein-micelle, proteoliposome, and protein-bicelle samples were prepared according to procedures described previously (20, 21). For concentration-dependent measurements several batches of samples with a molar ratio of SDS to protein varying over the range of 150 to 2000 were prepared by either changing the protein or SDS concentration. For these measurements we used proteins with spin labels at sites 24/61 or 24/72. Protein concentrations span from 20 to 100 μ M. SDS concentration was varied over the range of 5 to 60 mM.

Doubly spin-labeled 24/61 mutants of all protein variants were prepared in LPPG micelles with protein/LPPG concentrations of 60 μ M/40 mM, 60 μ M/80 mM, and 120 μ M/40 mM. Protein concentrations of 50 and 120 μ M for all α S variants were employed in the case of bicelles. The bicelle solution contained 162 mM total phospholipid concentration.

All samples for ESR spectroscopy measurements were made using D₂O buffers at pD 7.4 (uncorrected pH meter reading) and 100 mM NaCl with the subsequent addition of 10% (weight) glycerol-d₈ to bicelles samples and 30% (weight) to SDS and LPPG samples. As a control, we studied bicelle-bound WT α S with spin labels at positions 24/61 in both non-deuterated and deuterated phospholipids, and no differences were noted.

To estimate the extent of protein crowding on the surface of liposomes, we considered that a freely rotating protein molecule requires a disc of surface area corresponding to that of a circle with a radius equal to the maximum dimension of the protein, which for α S is about 15 nm in the extended helix conformation. Given the average liposome radius of 30 nm, $\sim 4\pi r_{\text{lipo}}^2 / \pi r_{\text{syn}}^2 = 16$ freely rotating α S molecules could coexist on the liposome surface.

RESULTS

Inter-spin Distances in Free State (D₂O:Glycerol-d₈ Medium)

To characterize the spatial extent of the highly disordered free state of α S, we used pulsed dipolar ESR spectroscopy employing the DEER pulse sequence to measure intramolecular distances between paramagnetic spin labels attached to

selected residues in the WT protein and also of PD-associated mutants A30P, A53T, and E46K (Fig. 1). Three different doubly spin-labeled cysteine mutants of each protein variant were examined: 24/61, 24/72, and 24/83. One spin label was attached at position 24, located in the N-terminal domain of the protein, and a second spin label was attached to a site at the very beginning (position 61) or the middle part (positions 72 or 83) of the NAC domain. Fig. 2 illustrates the time domain data and extracted distance distributions for WT and mutant α S. For all doubly spin-labeled proteins we observed a broad distribution of distances between spin labels, which could be interpreted as a superposition of dipole-dipole interactions between spin labels in individual protein molecules sampling an ensemble of conformations. Theoretically there are several sources of spectral broadening in pulsed dipolar spectroscopy (34), which include random mutual orientation of the spin labels, and a limited resolution due to the finite length of sampling interval also should be taken into account (29, 34, 35). However, for the highly dynamic free state of α S, we consider protein flexibility to be the primary source for the observed signal broadening. Where appropriate, we further quantified the observed distance distributions by approximating the distance distributions obtained by Tikhonov regularization using sums of up to two Gaussians, as illustrated in Fig. 2. The values of inter-spin distances and the widths of the distributions, as obtained from the modeling, are summarized in Table 1.

Our results show a similar overall behavior among all α S variants in terms of the distance distributions measured between spin labels attached to the same positions in the polypeptide chains. Interestingly, for the 24/61 and 24/72 pairs of spin labels, we observed bimodal distance distributions in each case, which were resolved by the two Gaussians approximation to have maximally probable distances ranging, among the four α S variants, from 3.2 to 3.6 and 5.0 to 5.2 nm for 24/61 and 3.5 to 4.2 and 5.3 to 6.1 nm for 24/72. For the 24/83 pair of spin labels, we observed a single maximally probable distance for all variants ranging from 3.6 to 4.1 nm (Table 1).

To better understand the structural properties of α S in solution, we considered polymer models previously employed in the analysis of protein structure (36–38). For polypeptide chains obeying random-flight statistics (Gaussian chain), the expected average mean square distance between two points (putative end-to-end distance) is $\langle R^2 \rangle = nl^2 + 2L^2$, where n is the number of chain segments (residues), l is the length of a segment (length of residue, generally taken to be 0.38 nm), and $2L^2$ is a term for two spin labels with a length of 0.8 nm. Straightforward calculations show that when spin labels are attached at positions 24/61, 24/72, and 24/83 in the proteins studied the expected values for spin-spin distances according to this model are 2.6, 2.9, and 3.1 nm, respectively. These calculated distances are somewhat smaller than the lower of the experimentally measured maximally probable distances (3.2–3.6, 3.5–4.2, and 3.6–4.1 nm for the 24/61-, 24/72-, and 24/83-labeled proteins, respectively, see Table 1), suggesting that this model does not describe adequately the structural properties of α S in solution, most likely as a result of some local stiffness of the polypeptide chain. We next applied a model that accounts for chain stiffness (see supplemental materials), which previously showed good

Helix Interconversion of α -Synuclein

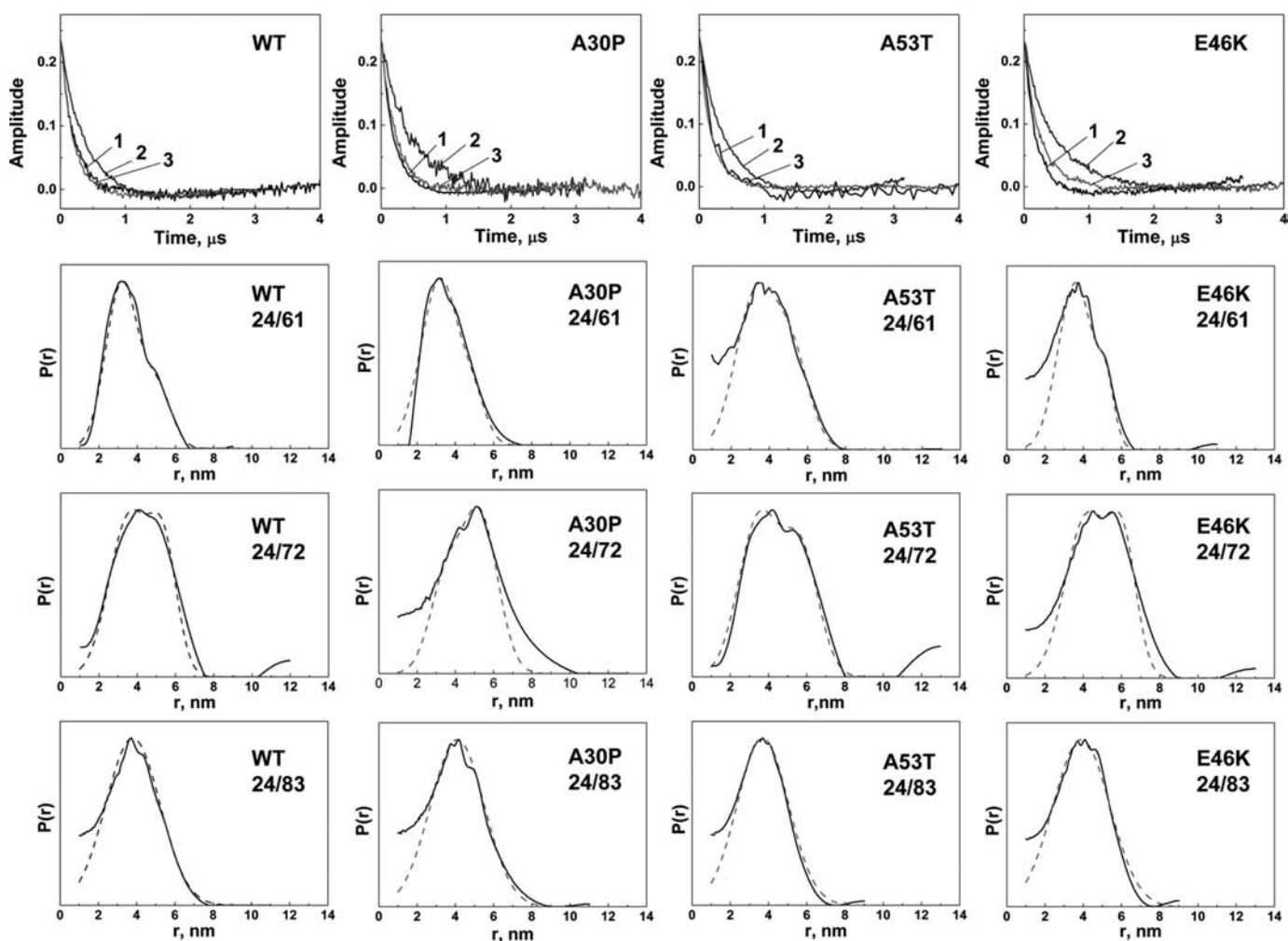


FIGURE 2. Experimental time domain data (top) and corresponding distance distributions for WT α S and its PD-linked mutants for three spin-labeled variants 24/61 (curve 1 in top panels), 24/72 (curve 2 in top panels), and 24/83 (curve 3 in top panels). The figure shows the data from the measurements on 100 μ M total protein concentration in 1:1 D₂O:Gly-d8. The distances were reconstructed by the Tikhonov regularization method with an additional refinement made by using MEM, as appropriate. The α S variant and spin label sites are indicated on each panel. The two Gaussian approximations to the experimental distance distributions are plotted by dashed lines. Parameters found from the Gaussians fits are given in Table 1.

TABLE 1

Two Gaussian model fitting parameters (R , ΔR , and percentages) used to approximate distance distributions for WT α S and its PD-linked mutants for three double cysteine mutants, 24/61, 24/72, and 24/83

All proteins were dissolved in 1:1 D₂O:Gly-d8, pD 7.4. Protein concentration was 100 μ M.

Labeled sites	Protein ^a											
	WT			A30P			A53T			E46K		
	R	ΔR	%	R	ΔR	%	R	ΔR	%	R	ΔR	%
24/61	3.2	2.0	78	3.2	2.3	88	3.3	2.5	67	3.6	2.2	88
	5.1	1.7	22	5.0	1.5	12	5.2	2.2	33	5.2	1.0	12
24/72	3.6	2.5	68	3.5	2.0	35	3.5	2.5	60	4.2	2.7	69
	5.4	1.7	32	5.3	2.2	65	5.7	2.2	40	6.1	1.7	31
24/83	3.8	3.3	100	4.1	3.3	100	3.6	3.2	100	3.9	3.5	100

^a The percentages have been estimated by fitting to sums of two Gaussians. Gaussian position, R , and full width at half-maximum, ΔR , are given in nanometers.

agreement with NMR paramagnetic relaxation enhancement data in the highly charged C-terminal tail of α S (27), whereas at the same time indicating that the N-terminal lipid-binding domain of the protein was more compact than predicted. This model yields expected values for spin-spin distances of 6.6, 7.7, and 8.6 nm for the three different spin-probe pairs. These distances are higher than the shorter of our experimentally observed values (3.2–3.6, 3.5–4.2, and 3.6–4.1 nm for the 24/61, 24/72, and 24/83 labeled proteins, respectively) indicat-

ing, in agreement with the NMR paramagnetic relaxation enhancement data (27), that the lipid-binding domain samples conformations that are considerably more compact than the random coil model. The calculated distances are more similar to, but still slightly larger than, the longer distances observed in the experimental distance distribution (5.0–5.2 and 5.3–6.1 nm for 24/61- and 24/72-labeled proteins, no longer distance was observed for 24/83-labeled protein) suggesting that some fraction of the protein ensemble may sample conformations

that are more consistent with those described by this statistical model. For the 24/83 pair, the calculated distance, 8.6 nm, is at the limit of our current measurement capability, which could explain why a long distance was not observed in the corresponding data.

Inter-spin Distances in Membrane-bound α S

Proteins Bound to SDS and LPPG Micelles—Micellar detergents have often been used as membrane mimetics capable of inducing native structure in membrane-binding proteins, despite their activity as protein denaturants (*e.g.* Refs. 39–41). In the case of α S, NMR studies of the protein bound to spheroidal SDS micelles indicated a highly helical structure in the lipid-binding domain of the protein (residues \sim 1–100) consisting of two helices separated by a non-helical linker region (17, 18) with no contacts detected between the helices (19, 26). Pulsed dipolar ESR spectroscopy was also applied to directly measure long inter-helical distances in the spheroidal SDS micelle-bound state of α S, with results that confirmed the broken helix structure proposed from NMR (20). Moreover, ESR experiments performed using non-denaturing lysophospholipid micelles instead of SDS revealed that the anti-parallel broken helix topology was preserved in the context of biologically relevant phospholipids (20). However, it was clearly shown that the conformation of α S depends on the geometry of the surface to which it is bound. In fact, subsequent ESR work (21, 22), confirmed by yet more recent FRET studies (23, 24), demonstrated that WT α S adopts a continuous and extended helical conformation when bound to lipid vesicles or bicelles, as well as to rod-like SDS micelles. Several of these studies also indicated that considerable flexibility is retained in both the broken and extended helix forms of α S, and furthermore, suggested that these two conformations of α S can interconvert under some conditions. Here we undertook a study to characterize this interconversion for both the WT- and PD-linked mutant proteins.

We initially applied DEER to WT α S spin labeled at positions 24/61 at a protein concentration of 100 μ M and detergent concentrations well above the expected critical micelle concentration of around 1 mM (25, 42) that, based on previous studies (25, 43, 44), are associated with the presence of either spheroidal (40 mM SDS) or cylindrical (450 mM SDS) micelles. We obtained distances corresponding to the broken and extended helix states (not shown), respectively, as expected based on previous ESR studies of α S at these SDS concentrations (20, 21). To visualize the transition between the two conformations in greater detail, we began a series of measurements at varying SDS concentrations, but using lower protein concentrations (20 and 40 μ M) to conserve material. Surprisingly, we found that different protein concentrations at a fixed detergent concentration led to different distance distributions, with lower protein concentrations resulting in distances indicative of the extended helix state and higher protein concentrations leading to the broken helix state (Fig. 3). This suggested that detergent-to-protein ratio, rather than just absolute detergent concentration, can influence the conformation adopted by α S. A separate titration varying protein concentration from 100 to 20 μ M at a fixed SDS concentration (40 mM) confirmed this obser-

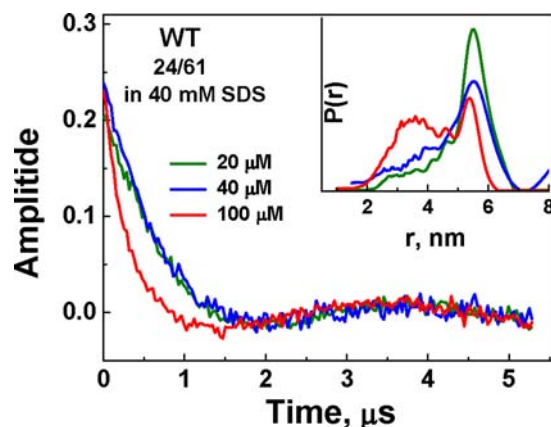


FIGURE 3. Experimental time domain data and respective distance distributions for WT α S spin-labeled at positions 24 and 61 at three protein concentrations (20, 40, and 100 μ M) and a fixed SDS concentration (40 mM). The distances were reconstructed by the Tikhonov regularization method and further refined by MEM. Protein concentrations are as indicated in the figure.

vation (supplemental Fig. S1 and Table S1). To further explore the transition of the protein between the two states, we applied DEER to different doubly spin-labeled forms of WT, as well as A30P, E46K, and A53T α S at a fixed protein concentration and varying detergent-to-protein ratios in the range of 125 to 1500. The extensive set of measurements and reconstructed distance distributions for the 24/61 and 24/72 spin label pairs for all protein variants is shown in Fig. 4. The distance distributions we observed were clearly sensitive to the detergent-to-protein ratio. In particular, at the lowest SDS concentrations, distances of around 3–4 nm, indicative of the broken helix state, predominated, whereas at the highest SDS concentrations distances of about 5–6 nm for the 24/61 labels and 6–7 nm for the 24/72 labels predominated, indicating the extended helix conformation. Importantly, even the highest SDS concentration used (60 mM) is below the concentrations ($>$ 200 mM) at which SDS is expected to spontaneously transition from spheroidal to cylindrical micelles (25, 44).

Both the shorter and longer distances we observed are indeed consistent with inter-helix distances previously observed for the broken helix (20) and extended helix (21) forms of the protein. Given this agreement, we again analyzed these distance distributions by fitting them to two Gaussians, as shown in Fig. 4 (*dashed lines*). Model parameters from the fits are summarized in Tables 2 and 3 and the extracted populations of the extended helix state for each condition are plotted in Fig. 5. We note that the estimated populations are highly reproducible (to within \sim 5% error) for different samples prepared identically using the same protein stock solutions (see supplemental materials). Thus, the variability in the populations observed in Fig. 5, both between α S variants, and between samples labeled at positions 24/61 *versus* 24/72, is unlikely to reflect errors in the measurement. Instead such differences must reflect either actual differences in the behavior of the different variants or the differently labeled proteins, or other sources of experimental error. We believe that errors in protein concentration, which influence the calculated detergent-to-protein ratio, are a primary source of experimental error, and unfortunately preclude any definitive conclusions

Helix Interconversion of α -Synuclein

regarding differences between the protein variants. Importantly, we note that although the data for the 24/72-labeled proteins never achieve as high a population of the extended helix state as observed for the corresponding conditions using 24/61-labeled proteins, we know that both types of labeled proteins are able to transition fully to the extended helix state at

very high detergent-to-protein ratios based on our previously studies of the WT protein (21).

We also note that a few of the distance distributions in Fig. 4 (as well as in subsequent figures discussed below) contain components that extend to shorter distances, well below 2 nm. We believe that this effect is an artifact that likely arises from the combination

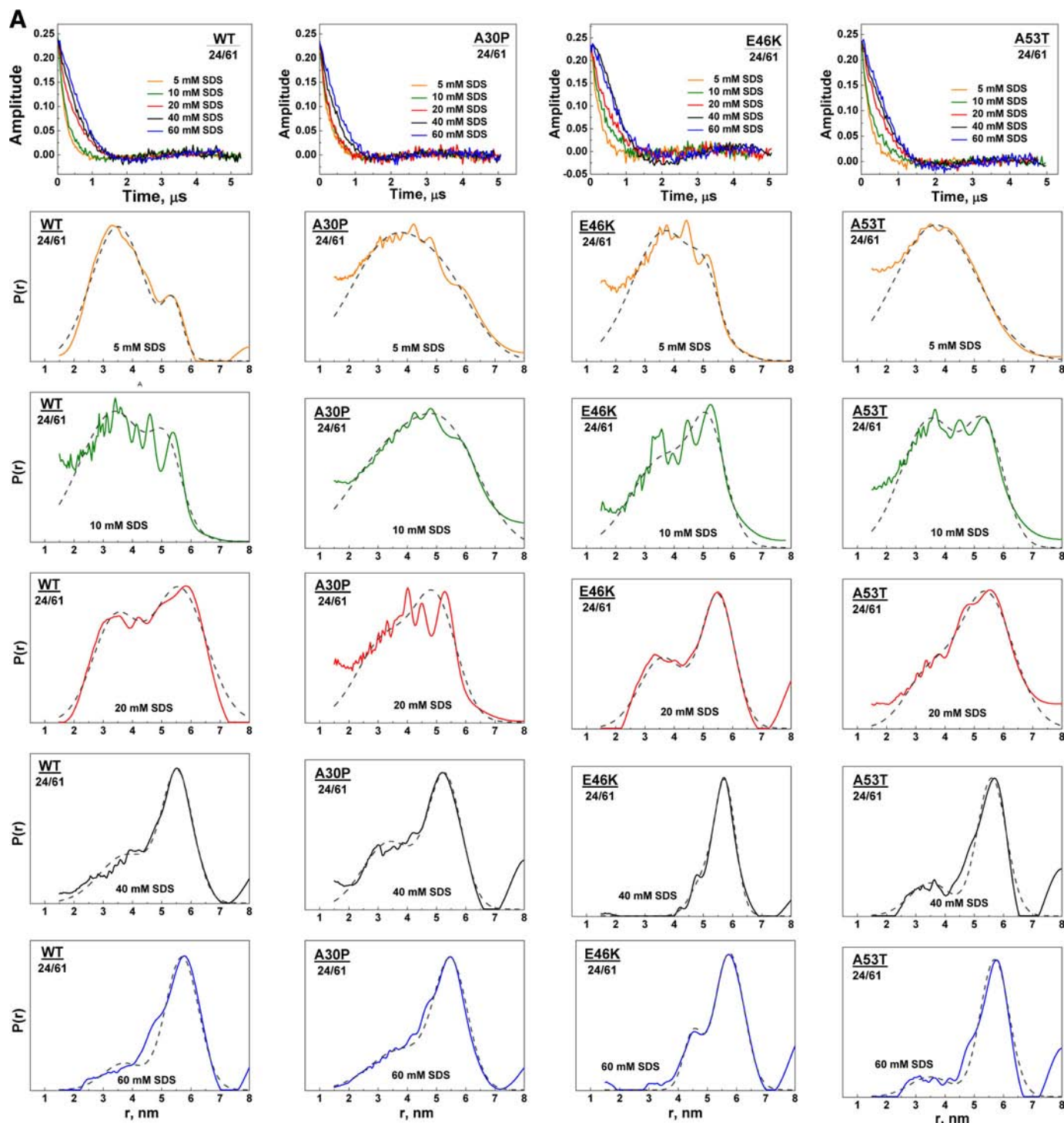


FIGURE 4. Experimental time domain data and their corresponding distance distributions for WT α S and its PD-linked mutants spin-labeled at positions 24 and 61 at SDS concentrations of 5 to 60 mM (panel A) or spin-labeled at positions 24 and 72 at SDS concentrations of 5 to 40 mM (panel B). Distances initially reconstructed using the Tikhonov L-curve method were used as seeds for MEM with automatic baseline correction for further refinement. The total protein concentration was 40 μ M in all cases. SDS concentrations are shown in each panel. Two Gaussian approximations to the experimental distance distributions were fit by varying the average distance, the distribution widths and the fractional population associated with each distance. The envelope of the best two Gaussian fit is plotted in each case using *dashed lines*. The average distances and standard deviations extracted from the fits are compiled in Tables 2 and 3.

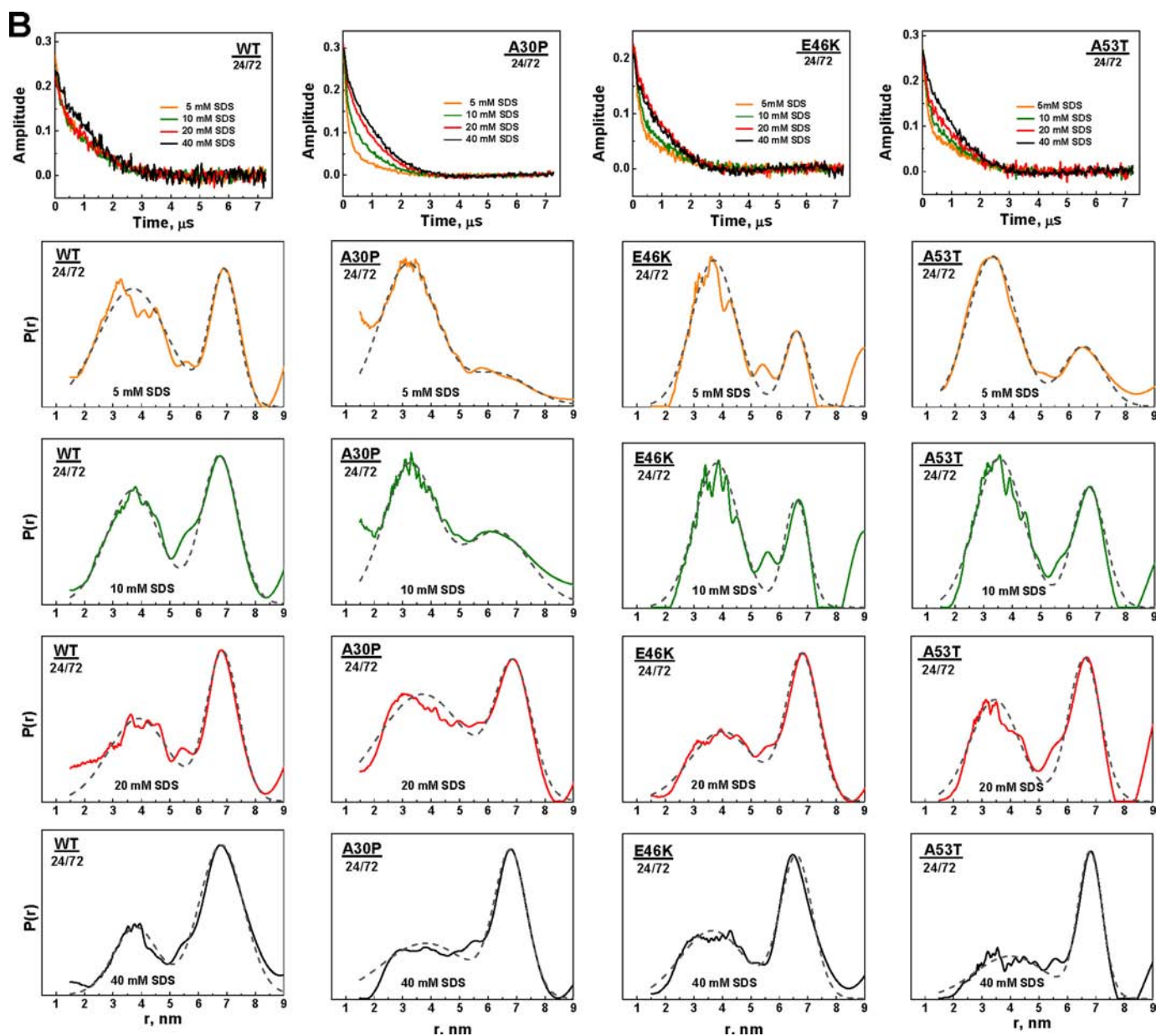


FIGURE 4—continued

TABLE 2

Two Gaussian model fitting parameters (average distance, R , and full width at half-maximum, ΔR , in nm) used to approximate distance distributions for α S and its PD-linked mutants, using protein doubly spin-labeled at positions 24 and 61

The protein was reconstituted at 40 μ M into SDS solutions at pD 7.4, 100 mM NaCl with SDS concentrations in range of 5 to 60 mM. Protein-to-detergent molar ratios are as indicated.

[SDS]	[Protein]/ [SDS]	Protein							
		WT		A30P		E46K		A53T	
		R	ΔR	R	ΔR	R	ΔR	R	ΔR
5 mM	1:125	3.5	2.2	3.5	3.3	3.7	2.7	3.7	3.3
		5.4	0.75	5.5	2.3	5.1	1.0	4.7	2.0
10 mM	1:250	3.4	2.8	3.5	3.5	3.7	2.7	3.5	2.3
		5.2	1.2	5.5	2.7	5.2	1.3	5.4	1.5
20 mM	1:500	3.4	1.8	3.3	2.3	3.6	1.8	3.4	1.8
		5.6	2.2	5.0	1.7	5.5	1.3	5.4	2.2
40 mM	1:1000	3.8	2.2	3.4	2.2	5.0	1.0	3.5	1.7
		5.55	1.25	5.3	1.3	5.75	0.8	5.6	1.2
60 mM	1:1500	3.7	1.7	3.8	2.5	4.5	0.75	3.5	1.7
		5.7	1.3	5.5	1.3	5.75	1.2	5.7	1.2

of relatively low signal-to-noise and the difficulty of obtaining accurate distances below 2 nm using DEER measurements (29, 35, 45). The fact that the presence of these shorter distance components in the data appears to be random with respect to protein variant or sample conditions supports our conclusion that they are artifacts. We also note that we previously used singly spin-labeled α S to rule out the possibility that detergent induces synuclein aggregation in our samples (20). We further examined this possibility by collecting data for samples in which doubly spin-labeled protein was diluted with unlabeled protein (supplemental Fig. S2 and Table S2). We find that our results are independent of spin label concentration, indicating that the observed distributions do not reflect inter-molecular distances and that the protein is therefore not aggregated under our conditions.

We also measured inter-spin distances for the three PD-associated mutants A30P, E46K, and A53T, with spin probes at

Helix Interconversion of α -Synuclein

TABLE 3

Two Gaussian model fitting parameters (average distance, R , and full width at half-maximum, ΔR , in nm) used to approximate distance distributions for α S and its PD-linked mutants, using protein doubly spin labeled at positions 24 and 72

The protein was reconstituted at 40 μ M into SDS solutions at pD 7.4, 100 mM NaCl with SDS concentrations in range of 5 to 40 mM. Protein-to-detergent molar ratios are as indicated.

[SDS]	[Protein]/[SDS]	Protein							
		WT		A30P		E46K		A53T	
		R	ΔR	R	ΔR	R	ΔR	R	ΔR
5 mM	1:125	3.7	2.8	3.2	2.3	3.7	1.8	3.3	2.0
		6.9	1.2	6.3	2.7	6.6	1.0	6.5	1.7
10 mM	1:250	3.7	2.2	3.25	2.2	3.8	1.8	3.55	2.0
		6.75	1.5	6.3	2.7	6.6	1.0	6.7	1.3
20 mM	1:500	3.9	2.5	3.7	3.7	4.0	2.7	3.45	2.0
		6.85	1.3	6.9	1.5	6.8	1.3	6.6	1.3
40 mM	1:1000	3.8	1.8	3.8	3.7	3.65	2.7	4.0	3.0
		6.8	1.8	6.8	1.3	6.6	1.3	6.8	1.0

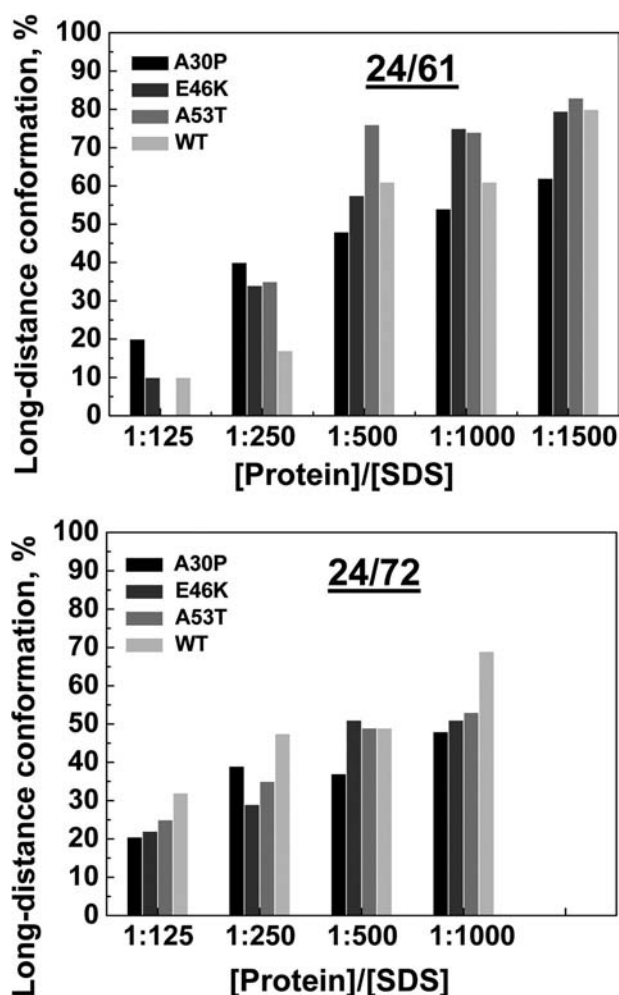


FIGURE 5. Estimated fractional populations associated with the longer of the two distances extracted from the two Gaussian fits shown in Fig. 4. The longer distance in each case is in good agreement with that previously determined for the extended helix conformation of the protein for proteins labeled both at positions 24 and 61 (upper panel) and 24 and 72 (lower panel) (21). Thus the extracted population can be used as an estimate of the fraction of the protein adopting the extended helix state. The results, plotted as a function of protein to SDS ratio for each protein variant, demonstrate that the population of the extended helix conformation increases with increasing detergent concentration. The errors in the extracted populations are estimated to be on the order of 10%, including uncertainties in protein concentrations, as well as errors arising from data acquisition and analysis.

positions 24/61, at a protein concentration of 100 μ M, and an SDS concentration of 450 mM (Fig. 6). For the E46K and A53T mutants, single distances of 5.6 (ΔR 1.5) and 5.7 (ΔR 1.2) nm, respectively, were observed, consistent with the expected and previously measured (21) distance characteristics of the extended helix conformation. For these mutants, we observed satellite peaks on both sides of the main peak. These are most likely a result of an angular dependence in the dipole-dipole interaction, which appears to be incompletely averaged at these conditions, indicating a relatively rigid protein conformation. A similar effect was observed in recent studies of micelle-bound monoamine oxidases (30). For the A30P mutant, a similar maximally probable distance of 5.5 (ΔR 2.3) nm, but a broader distance distribution suggests a more dynamic ensemble of conformations.

Finally we performed distance measurements for the three PD-linked α S mutants bound to LPPG micelles with spin labels at the 24/61 positions. Under all protein and LPPG concentrations studied, a single maximally probable distance of around 4.5 nm was found (Fig. 7), consistent with previous measurements for the WT protein (20), and indicating the formation of the broken helix conformation.

It is noteworthy that the distance distributions obtained in our studies of both micelle-bound (see above) and membrane-bound (see below) α S are unusually broad. Although the flexibility of the nitroxide spin labels is expected to introduce a level of uncertainty into the measurement, this effect is not expected to be larger than \sim 1 nm (34, 45–47). For measurements of the very long distances associated with the extended helix conformation, long signal acquisition times are required, leading to a decreased signal-to-noise ratio and potentially contributing to a larger uncertainty in the distance reconstruction algorithm (34). However, we believe the primary contribution to the breadth of the distance distributions is most likely to be the innate flexibility of the linker region in both the broken and extended helix conformations, which has been previously documented both in our own work (20, 21) and that of others (19, 25), and which leads to relative motions of the helix-1 region with respect to the helix-2 region in both the micelle and vesicle-bound protein.

Proteins Bound to Liposomes and Bicelles—Recently (21) we reported, based on long-distance constraints from DEER spectroscopy, that *in vitro* WT α S forms a single extended helix when it is bound to liposomes and bicelles with a high content of charged phospholipid. Here we extend our studies of the WT protein to include additional longer distance measurements, as well as analogous measurements for the three PD-linked mutations using four doubly labeled cysteine sites: 50/72, 24/61, 24/72, and 24/83.

Liposomes were prepared by sonication (see “Experimental Procedures”) and were determined by electron microscopy to have an average diameter of about 60 nm. Estimating that each phospholipid molecule occupies 0.5 nm² of surface area, a 60-nm spherical liposome contains 22,619 phospholipid molecules. We used protein and phospholipid concentrations of 30 μ M and 60 mM, respectively, for these measurements, leading to a protein:liposome ratio of about 10:1. Note that the surface of a 60-nm liposome can accommodate \sim 16 freely rotating copies of a 15-nm long helix (roughly the dimensions of the extended

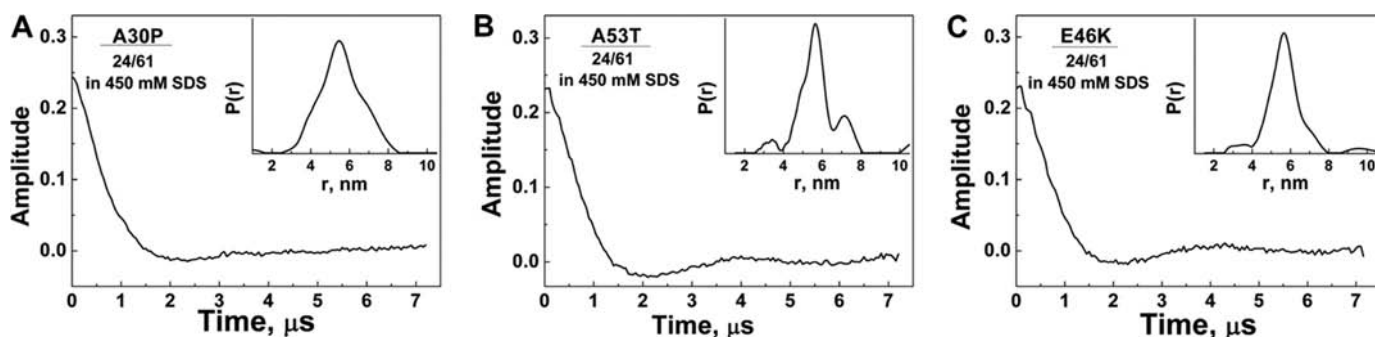


FIGURE 6. Experimental time domain data and corresponding distance distributions from α S PD mutants A30P (A), E46K (B), and A53T (C) bound to rod-like micelles at 450 mM SDS. Proteins were spin labeled at positions 24 and 61. The total protein concentration was 100 μ M. Distances were reconstructed by the L-curve method. Average distances of 5.5, 5.6, and 5.7 nm were determined for the A30P, E46K, and A53T mutants, respectively.

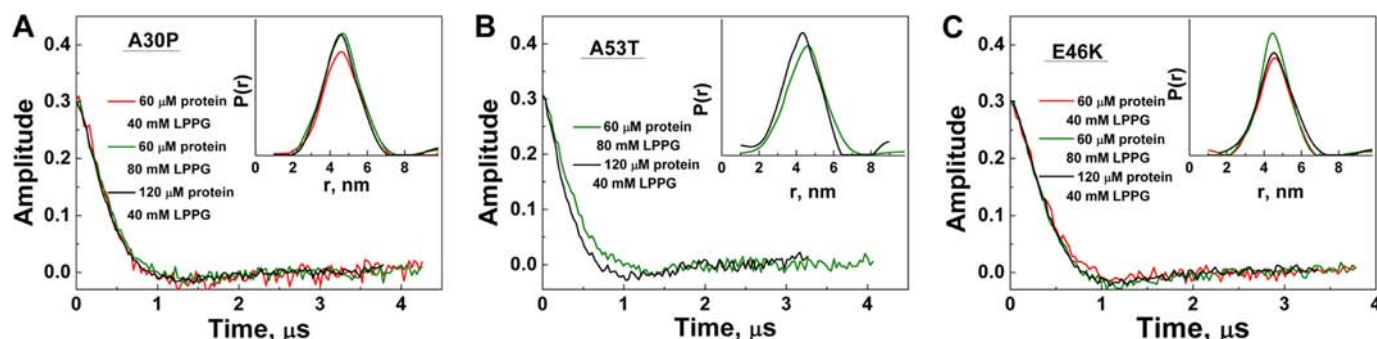


FIGURE 7. Experimental time domain data and corresponding reconstructed distances from PD mutants A30P (A), E46K (B), and A53T (C), bound to LPPG micelles, with spin labels residing at positions 24 and 61. The total protein/LPPG concentrations used are 60 μ M/40 mM (red), 60 μ M/80 mM (green), and 120 μ M/40 mM (black). Distances were reconstructed by the L-curve method.

helix form of α S), that is to say the α S molecules are not overly crowded under our conditions (see “Experimental Procedures”). For spin labels attached at positions 50/72 in α S, the label sites are expected to be connected by a continuous helical conformation in either the broken helix or extended helix forms of the protein. For these samples, maximally probable distances of about 3.4 nm were measured in all protein variants (Fig. 8A and Table 4), which is very close to the expected value of 3.3 nm for the length of a 22-residue ideal α -helix.

For labels at sites 24/61, 24/72, and 24/83, distances of about 5.5, 7, and 8.7 nm, respectively, were determined (*cf.* Fig. 8, B and C), which are also consistent with a continuous helical structure between each of the spin-label pairs for each protein variant. The observed distances are compiled in Table 4.

Measurements made in the presence of bicelles revealed similar distances to those observed in liposomes (Fig. 9 and Table 4) at protein concentrations of 50 μ M, but the A30P mutant gave a much broader distance distribution than the other variants. Furthermore, at higher protein concentrations (120 μ M) the data remained similar for the WT, E46K, and A53T variants, but A30P showed a distribution with a shorter maximally probable distance, resembling that observed for the protein free in solution, suggesting that at these concentrations, a significant fraction of the A30P mutant is unbound, an observation consistent with the previously reported reduced affinity of this mutant for lipid membranes (16, 48–50).

DISCUSSION

Compactness and Interconversion of Free α S—The results we obtain for all four α S variants when free in solution (Fig. 2 and

Table 1) indicate a highly flexible ensemble of conformations, consistent with many other results documenting that free α S is highly disordered (7, 8, 51). In addition, we observed that the spatial extent of at least part of the ensemble sampled by the lipid-binding domain of the protein is less than that which would be expected for a Gaussian random coil with a persistence length similar to that of simple amino acid homopolymers. These results are similar to those reported in a previous ESR study of WT free α S (52) and are also consistent with previous studies (53, 54), and in particular supports prior NMR PRE-based observations showing that this region of α S is more compact than would be expected based on the same statistical model (27). Interestingly, however, our data also document the existence of more highly extended conformations, with distance parameters that more closely approach those predicted by the statistical model. This suggests that the interactions responsible for the compact conformations of the protein are likely transient in nature, causing the protein to fluctuate between extended and compact states. This conclusion is again consistent with prior NMR studies indicating an absence of persistent long range contacts in the protein (55) as well as with recent electron transfer experiments documenting dynamic long range contacts (56, 57). Notably, the longer distances we have observed were not detected in prior ESR measurements of the free protein. A possible explanation could be found in the different experimental conditions and/or different levels of pulsed ESR instrumentation sensitivity at longer distances.

With respect to the effects of PD-linked mutations on the free state of α S, some reports have suggested that these muta-

Helix Interconversion of α -Synuclein

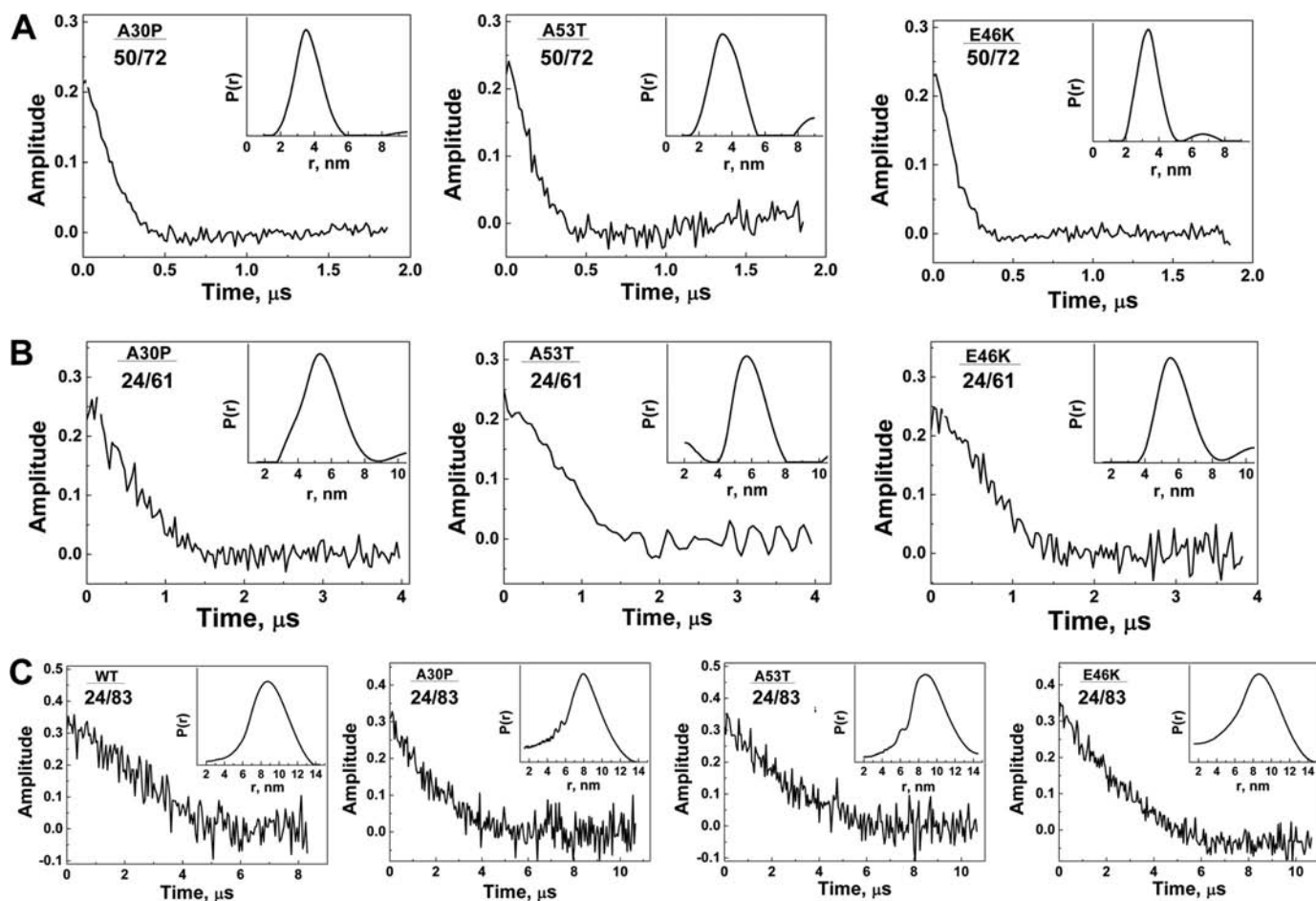


FIGURE 8. Experimental time domain data and corresponding distance distributions. *A*, spin labels at positions 50 and 72 in α S PD mutants A30P, E46K, and A53T; *B*, spin labels at positions 24 and 61 in PD mutants A30P, E46K, and A53T; and *C*, spin labels at positions 24 and 83 in WT α S and the three PD mutants. Distances were reconstructed by the L-curve method. The proteins were reconstituted in DMPC/DMPG liposomes. The total protein concentration was 30 μ M. In the case of proteins with spin-labeled sites 24 and 83, 70% deuterated proteins were reconstituted into DMPG-d54, DMPC-d67 proteoliposomes using deuterated buffers.

TABLE 4

Maximally probable distance, R , and full width at half-maximum, ΔR , in nm, of the distance distributions obtained using spin labels at positions 50/72, 24/61, 24/72, and 24/83 in WT α S and PD associated mutants A53T, E46K, and A30P in liposomes and bicelles

The expected distances for an ideal α -helix connecting residues 50/72, 24/61, 24/72, and 24/83 are 3.3, 5.55, 7.2, and 8.85 nm, respectively. All distances were reconstructed by the L-curve method and refined by MEM as necessary.

Protein	Double mutant	Mimetic membrane			
		Liposomes		Bicelles	
		R	ΔR	R	ΔR
WT	50/72	3.5 ^a	0.8	3.8 ^a	0.9
	24/61	5.5 ^a	2.1	5.8 ^a	1.2
	24/72	6.9	2.4	7.5 ^a	1.9
	24/83	8.7	3.0	8.05	1.9
A53T	50/72	3.4	2.2	3.7	1.7
	24/61	5.7	1.9	5.7	1.8
	24/72	6.8	2.8	6.9	3.7
	24/83	8.7	4.1	N/A ^b	
E46K	50/72	3.3	1.4	3.2	0.8
	24/61	5.5	2.2	5.7	1.8
	24/72	N/A		6.8	2.5
	24/83	8.8	4.6	N/A	
A30P	50/72	3.5	1.9	3.8	1.5
	24/61	5.3	2.6	5.4 ^c	2.5
	24/72	6.9	3.5	6.8	2.8
	24/83	8.0	3.9	N/A	

^a Distances from Georgieva *et al.* (21).

^b N/A, not available.

^c For lower protein concentration (50 μ M, see text).

tions may alter long range contacts between the C-terminal tail and the N-terminal lipid-binding domain of the protein (58, 59). The experiments we describe here monitor the compactness of the lipid-binding domain of the protein, and within the accuracy of our results, no significant differences were found in the spatial extent of this domain of the WT and three PD-linked mutations.

Transition between the Broken and Extended Helix States in the Presence of Detergent—Initial NMR studies of the structure of α S in the presence of detergent micelles were performed using SDS concentrations and conditions that, in the absence of protein, result in the formation of spheroidal micelles (8, 17). At the protein concentrations used in those experiments it was found, indeed, that NMR spectral properties, as well as the observed broken helix protein conformation, were consistent with the presence of spheroidal micelles, and this was further confirmed in subsequent NMR (19) and ESR (20) experiments. More recently, a careful study of α S structural transitions using CD spectroscopy revealed that at higher detergent concentrations, where SDS is known to form cylindrical rod-like micelles, a somewhat more highly helical form of the protein was observed (25), which was posited to be, and subsequently shown to be (21), the previously proposed (8) extended helix structure of the protein.

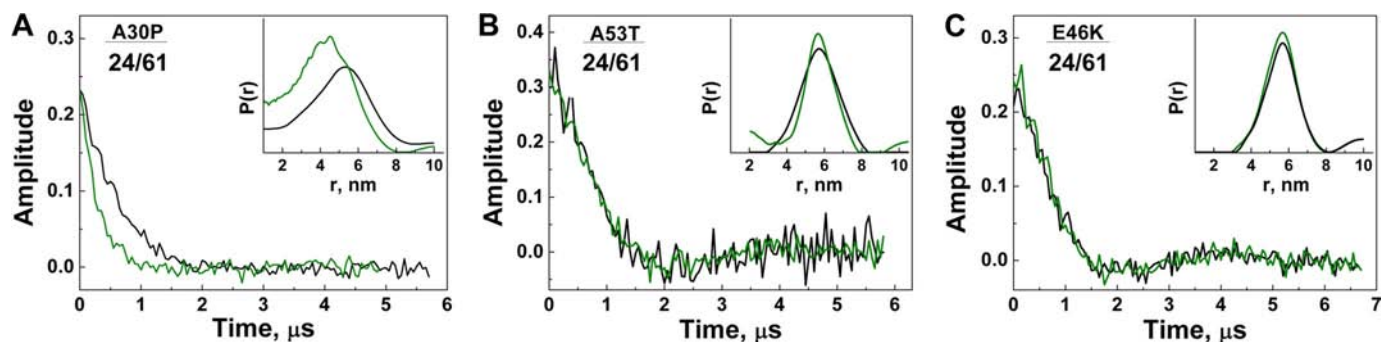


FIGURE 9. Experimental time domain data and corresponding distance distributions from PD mutants A30P (A), E46K (B), and A53T (C) bound to DMPC/DMPG/DHPC bicelles. Spin labels were at positions 24 and 61. The total protein concentrations used were 50 μ M (black) and 120 μ M (olive). Distances were reconstructed by the L-curve method with MEM refinement.

Subsequent studies of detergent- and vesicle-bound α S reported observations of both the extended helix (21–24) and broken helix (21, 23, 60, 61) forms of the protein in both contexts, leading to the suggestion by several groups (21, 23, 62) that the protein may indeed interconvert between the two conformations depending on its environment. Our results here show that the transition from broken helix to the extended helix form of the protein in the presence of detergent not only depends on the environment of the protein, *i.e.* the presence of spheroidal or rod-like micelles, but rather that the protein may potentially also influence its environment. This conclusion is based on our observation that at detergent concentrations (*e.g.* 40 mM) well above the critical micelle concentration of SDS under similar conditions (25, 42) but well below the threshold for spontaneous formation of cylindrical micelles (25, 44), the conformation we observe for the protein depends not only on the absolute concentration of SDS, but also on the relative concentrations of the protein and detergent (Figs. 3 and 4). Within the range of concentrations that we studied here, we observed that the broken helix form of the protein dominates at detergent-to-protein ratios below \sim 500, whereas the extended helix form of the protein prevails at higher ratios (Tables 2 and 3). It should be noted that this is approximately the number of detergent molecules needed to form a rod-like micelle as long as the extended helix α S conformation (\sim 14 nm). Furthermore, as pointed out previously (17), it is difficult to envision how the extended helix state of the protein could bind to a spheroidal micelle. Thus, it appears likely that the conformation of the protein is coupled to the topology adopted by the detergent. At present, however, we are not able to directly determine the shape of the micelles to which the protein is bound, limiting our ability to study how α S influences micelle topology. Nevertheless, a number of previous reports have shown that α S may influence detergent and membrane assembly and topology. Indeed, α S has been observed to influence the critical micelle concentration of SDS (42), to directly perturb lipid bilayer structure *in vitro* (63–66), and even to remodel membrane topology (67, 68). Such activities could be consistent with a number of studies showing that α S can influence the neurotransmitter release at synapses (69, 70) and may be directly involved in vesicle fusion pathways (71–73). The potential role of the interconversion of the protein between the broken and extended helix forms in mediating such effects remains to be

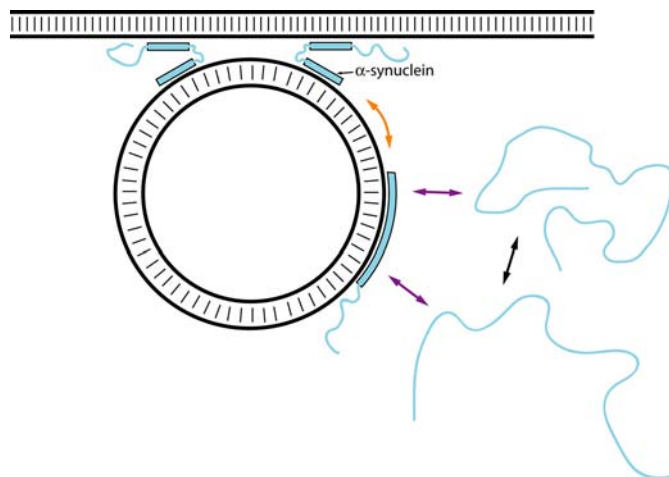


FIGURE 10. Hypothetical model of a possible *in vivo* context for the structural transitions of α S. The free state ensemble contains both compact and extended conformations (black arrow), which can convert to the synaptic vesicle-bound extended helix state (purple arrows). The extended helix state could in turn convert to a membrane-spanning broken helix state when the vesicle nears the plasma membrane (orange arrow). By spanning between synaptic vesicles and the plasma membrane, synuclein could play a role in regulating the stability and fusion of docked neurotransmitter-filled vesicles. PD-linked mutations retain the ability to populate all of these conformations. However, our data here are consistent with previous indications that the A30P mutation influences membrane binding by the protein (purple arrows) and also support a recent report (74) suggesting that A30P could alter the ability of the protein to convert between the broken and extended helix states (orange arrow), which could potentially alter or interfere with normal α S function.

explored, but we have proposed one specific model (62) in which this conversion process may play a role in regulating synaptic vesicle fusion by allowing the protein to bridge between different membranes (Fig. 10).

The interconversion of the broken helix and extended helix states of α S as a function of detergent-to-protein ratio does not appear to be obviously influenced by the presence of three PD-linked mutations. Interestingly, while this manuscript was under review, a study using FRET to monitor transitions in SDS-bound α S appeared and reported that the conversion of the A30P mutant to the extended helix conformation is somewhat inhibited (74). In our results (Fig. 5) the conversion of the A30P mutant to the extended helix form seems to slightly lag the other three variants in data obtained using both the 24/61- and 24/72-labeled proteins (more dramatically so in the former), with the transition from one form to the other occurring

Helix Interconversion of α -Synuclein

at a slightly higher detergent-to-protein ratio. However, the differences are not conclusive as they fall within our estimate of the uncertainty in the extracted populations. We have recently proposed that the observed interconversion may be involved in the normal function of α S (21, 62), as illustrated in Fig. 10. Thus, any α S mutation that alters the ability of the protein to interconvert between the extended and broken helix forms could, in principle, influence the normal function of the protein.

Influence of PD-linked Mutations on the Extended Helix Conformation of Bicelle- and Vesicle-bound α S—Our studies of bicelle- and liposome-bound α S further support our previous results documenting the presence of the extended helix conformation of the protein in these contexts (21). Indeed, we have now extended our measurements to include distances of up to 8.7 nm for α S labeled at the 24/83 positions (we believe to be the longest distance measured within a protein using pulsed ESR methods to date) (Fig. 8). All of the maximally probable distances we observe correspond to those that would be expected for a continuous α -helix connecting the two spin-label sites (Table 4). At the same time, most of the measurements have yielded broad distance distributions that suggest the presence of conformations with shorter distances, likely reflecting flexing of the single extended helix, either throughout its length or through more localized fluctuations of the linker region. Alternately, short distances could reflect the presence of some unbound protein within the samples, as has been observed in other studies of α S-lipid interactions (48) and that may result from the relatively weak affinity of the protein for lipid vesicles, estimated at $\sim 100 \mu\text{M}$ under our conditions (75).

We also examined, for the first time, the effects of the PD-linked α S mutations on the extended helix conformation of the vesicle-bound protein. For the E46K and A53T mutations, the data appear nearly identical to those obtained for the WT protein, suggesting that these mutations do not influence the structure of the vesicle- or bicelle-bound protein, and indeed do not appear to perturb the micelle-bound conformations of the protein either. This is consistent with prior NMR work on the broken helix state of the A53T variant (48, 76), although preliminary NMR characterization has suggested that the E46K mutation may influence the conformation of the linker region in the broken helix state (77). As suggested previously for A53T (48), any alteration of α S function by these mutations may be related to an effect on the interactions of the protein with other cellular components, such as other proteins, rather than on its interactions with lipids.

For the case of the A30P mutation, the previously reported lower affinity of this variant for lipid membranes (16, 48–50) is evident in our data at higher protein-to-lipid ratios, where a distance distribution characteristic of unbound protein was observed (Fig. 9). At lower protein concentrations, longer distances characteristic of the extended helix state were observed, but with a significantly broader distribution than for the WT and the other two mutants (Fig. 9), confirming that the A30P mutant retains the ability to bind to form the extended helix conformation, but suggesting a greater degree of flexibility or disorder than for the other protein variants. The fact that the control measurement of distances between sites 50 and 72 yielded very similar results for the A30P mutant as for all the

other α S variants (similar maximal distances and distribution widths), suggests that regions of the protein distant from the A30P mutation site are unaffected by the mutation. Instead, the additional flexibility implied by the data might result from more local structural perturbations. These could be confined to the immediate vicinity of the mutation site. Indeed, previous studies of this mutation in the broken helix conformation revealed increased disorder primarily confined to the vicinity of the mutation (48). However, subsequent studies (76) revealed that the effects of the A30P mutation in the broken helix state extended through the entire linker region between the two helices. Thus, it is possible that this mutation decreases the stability of the linker region in the extended helix state as well, leading to an increased flexibility and the broader distance distributions observed. Alternately, an increased population of free protein could contribute additional distances to the observed distribution beyond those already observed for WT and other mutant proteins. Although it is not possible to rule out any of these (or other) possibilities at present, some of our data for the A30P mutant at different SDS concentrations, as well as newly reported FRET data (74) suggest, as discussed above, that this mutation may decrease the propensity of the protein to adopt the extended helix state, supporting a model in which one of its effects may indeed be to influence the stability of the linker region structure.

Conclusions—1) The lipid-binding domain of the free state of α S fluctuates between random coil-like and more compact conformations, and this ensemble is not strongly influenced by the presence of PD-linked mutations.

2) The conformations that α S adopts in the presence of SDS micelles are not strictly determined by the pre-existing micelle topology. Instead, over a certain range of detergent concentrations, the detergent-to-protein ratio affects the distribution of the broken and extended helix protein conformations. This is consistent both with the ability of membranes to influence α S conformation and with the ability of α S to influence membrane structure.

3) All three PD-linked mutations retain the ability to adopt the extended helix state when bound to rod-like micelles or phospholipids bicelles and vesicles, but the A30P mutation leads to a decreased affinity and an increase in local disorder in this conformation of the protein. This disorder may extend into the linker region and thereby inhibit the conversion of the protein from the broken helix to the extended helix state; an effect that could influence the normal function of the protein.

REFERENCES

1. Maroteaux, L., Campanelli, J. T., and Scheller, R. H. (1988) *J. Neurosci.* **8**, 2804–2815
2. Ueda, K., Fukushima, H., Maslah, E., Xia, Y., Iwai, A., Yoshimoto, M., Otero, D. A., Kondo, J., Ihara, Y., and Saitoh, T. (1993) *Proc. Natl. Acad. Sci. U.S.A.* **90**, 11282–11286
3. Polymeropoulos, M. H., Higgins, J. J., Golbe, L. I., Johnson, W. G., Ide, S. E., Di Iorio, G., Sanges, G., Stenroos, E. S., Pho, L. T., Schaffer, A. A., Lazzarini, A. M., Nussbaum, R. L., and Duvoisin, R. C. (1996) *Science* **274**, 1197–1199
4. Spillantini, M. G., Schmidt, M. L., Lee, V. M., Trojanowski, J. Q., Jakes, R., and Goedert, M. (1997) *Nature* **388**, 839–840
5. Tofaris, G. K., and Spillantini, M. G. (2007) *Cell Mol. Life Sci.* **64**, 2194–2201

6. Waxman, E. A., and Giasson, B. I. (2009) *Biochim. Biophys. Acta* **1792**, 616–624
7. Weinreb, P. H., Zhen, W., Poon, A. W., Conway, K. A., and Lansbury, P. T., Jr. (1996) *Biochemistry* **35**, 13709–13715
8. Eliezer, D., Kutluay, E., Bussell, R., Jr., and Browne, G. (2001) *J. Mol. Biol.* **307**, 1061–1073
9. Uversky, V. N., and Eliezer, D. (2009) *Curr. Protein Pept. Sci.* **10**, 483–499
10. George, J. M., Jin, H., Woods, W. S., and Clayton, D. F. (1995) *Neuron* **15**, 361–372
11. Irizarry, M. C., Kim, T. W., McNamara, M., Tanzi, R. E., George, J. M., Clayton, D. F., and Hyman, B. T. (1996) *J. Neuropathol. Exp. Neurol.* **55**, 889–895
12. Kahle, P. J., Neumann, M., Ozmen, L., Muller, V., Jacobsen, H., Schindzielorz, A., Okochi, M., Leimer, U., van Der Putten, H., Probst, A., Kremmer, E., Kretzschmar, H. A., and Haass, C. (2000) *J. Neurosci.* **20**, 6365–6373
13. McLean, P. J., Kawamata, H., Ribich, S., and Hyman, B. T. (2000) *J. Biol. Chem.* **275**, 8812–8816
14. Davidson, W. S., Jonas, A., Clayton, D. F., and George, J. M. (1998) *J. Biol. Chem.* **273**, 9443–9449
15. Jo, E., McLaurin, J., Yip, C. M., St. George-Hyslop, P., and Fraser, P. E. (2000) *J. Biol. Chem.* **275**, 34328–34334
16. Perrin, R. J., Woods, W. S., Clayton, D. F., and George, J. M. (2000) *J. Biol. Chem.* **275**, 34393–34398
17. Bussell, R., Jr., and Eliezer, D. (2003) *J. Mol. Biol.* **329**, 763–778
18. Chandra, S., Chen, X., Rizo, J., Jahn, R., and Südhof, T. C. (2003) *J. Biol. Chem.* **278**, 15313–15318
19. Ulmer, T. S., Bax, A., Cole, N. B., and Nussbaum, R. L. (2005) *J. Biol. Chem.* **280**, 9595–9603
20. Borbat, P., Ramlall, T. F., Freed, J. H., and Eliezer, D. (2006) *J. Am. Chem. Soc.* **128**, 10004–10005
21. Georgieva, E. R., Ramlall, T. F., Borbat, P. P., Freed, J. H., and Eliezer, D. (2008) *J. Am. Chem. Soc.* **130**, 12856–12857
22. Jao, C. C., Hegde, B. G., Chen, J., Haworth, I. S., and Langen, R. (2008) *Proc. Natl. Acad. Sci. U.S.A.* **105**, 19666–19671
23. Ferreon, A. C., Gambin, Y., Lemke, E. A., and Deniz, A. A. (2009) *Proc. Natl. Acad. Sci. U.S.A.* **106**, 5645–5650
24. Trexler, A., and Rhoades, E. (2009) *Biochemistry* **48**, 2304–2306
25. Ferreon, A. C., and Deniz, A. A. (2007) *Biochemistry* **46**, 4499–4509
26. Bussell, R., Jr., Ramlall, T. F., and Eliezer, D. (2005) *Protein Sci.* **14**, 862–872
27. Sung, Y. H., and Eliezer, D. (2007) *J. Mol. Biol.* **372**, 689–707
28. Borbat, P. P., Crepeau, R. H., and Freed, J. H. (1997) *J. Magn. Reson.* **127**, 155–167
29. Borbat, P. P., and Freed, J. H. (2007) *Methods Enzymol.* **423**, 52–116
30. Upadhyay, A. K., Borbat, P. P., Wang, J., Freed, J. H., and Edmondson, D. E. (2008) *Biochemistry* **47**, 1554–1566
31. Jeschke, G., Koch, A., Jonas, U., and Godt, A. (2002) *J. Magn. Reson.* **155**, 72–82
32. Chiang, Y. W., Borbat, P. P., and Freed, J. H. (2005) *J. Magn. Reson.* **172**, 279–295
33. Chiang, Y. W., Borbat, P. P., and Freed, J. H. (2005) *J. Magn. Reson.* **177**, 184–196
34. Borbat, P. P., McHaourab, H. S., and Freed, J. H. (2002) *J. Am. Chem. Soc.* **124**, 5304–5314
35. Borbat, P. P., and Freed, J. H. (2007) *EPR Newsletter* **17**, 21–33
36. Flory, P. J. (1969) *Statistical Mechanics of Chain Molecules*, Wiley Interscience, New York
37. Fitzkee, N. C., and Rose, G. D. (2004) *Proc. Natl. Acad. Sci. U.S.A.* **101**, 12497–12502
38. Kohn, J. E., Millett, I. S., Jacob, J., Zagrovic, B., Dillon, T. M., Cingel, N., Dothager, R. S., Seifert, S., Thiyagarajan, P., Sosnick, T. R., Hasan, M. Z., Pande, V. S., Ruczinski, L., Doniach, S., and Plaxco, K. W. (2004) *Proc. Natl. Acad. Sci. U.S.A.* **101**, 12491–12496
39. Jaronec, C. P., Kaufman, J. D., Stahl, S. J., Viard, M., Blumenthal, R., Wingfield, P. T., and Bax, A. (2005) *Biochemistry* **44**, 16167–16180
40. Boettcher, J. M., Hartman, K. L., Ladrer, D. T., Qi, Z., Woods, W. S., George, J. M., and Rienstra, C. M. (2008) *Biochemistry* **47**, 12357–12364
41. Chill, J. H., Louis, J. M., Miller, C., and Bax, A. (2006) *Protein Sci.* **15**, 684–698
42. Necula, M., Chirita, C. N., and Kuret, J. (2003) *J. Biol. Chem.* **278**, 46674–46680
43. Rao, I. V., and Ruckenstein, E. (1987) *J. Colloid Interface Sci.* **119**, 211–227
44. Otzen, D. E. (2002) *Biophys. J.* **83**, 2219–2230
45. Banham, J. E., Baker, C. M., Ceola, S., Day, I. J., Grant, G. H., Groenen, E. J., Rodgers, C. T., Jeschke, G., and Timmel, C. R. (2008) *J. Magn. Reson.* **191**, 202–218
46. Hustedt, E. J., Stein, R. A., Sethaphong, L., Brandon, S., Zhou, Z., and Desensi, S. C. (2006) *Biophys. J.* **90**, 340–356
47. Bhatnagar, J., Freed, J. H., and Crane, B. R. (2007) *Methods Enzymol.* **423**, 117–133
48. Bussell, R., Jr., and Eliezer, D. (2004) *Biochemistry* **43**, 4810–4818
49. Jensen, P. H., Nielsen, M. S., Jakes, R., Dotti, C. G., and Goedert, M. (1998) *J. Biol. Chem.* **273**, 26292–26294
50. Jo, E., Fuller, N., Rand, R. P., St. George-Hyslop, P., and Fraser, P. E. (2002) *J. Mol. Biol.* **315**, 799–807
51. Bussell, R., Jr., and Eliezer, D. (2001) *J. Biol. Chem.* **276**, 45996–46003
52. Drescher, M., Godschalk, F., Veldhuis, G., van Rooijen, B. D., Subramaniam, V., and Huber, M. (2008) *ChemBioChem* **9**, 2411–2416
53. Morar, A. S., Olteanu, A., Young, G. B., and Pielak, G. J. (2001) *Protein Sci.* **10**, 2195–2199
54. Uversky, V. N., Li, J., Souillac, P., Millett, I. S., Doniach, S., Jakes, R., Goedert, M., and Fink, A. L. (2002) *J. Biol. Chem.* **277**, 11970–11978
55. Dedmon, M. M., Christodoulou, J., Wilson, M. R., and Dobson, C. M. (2005) *J. Biol. Chem.* **280**, 14733–14740
56. Lee, J. C., Gray, H. B., and Winkler, J. R. (2005) *J. Am. Chem. Soc.* **127**, 16388–16389
57. Lee, J. C., Lai, B. T., Kozak, J. J., Gray, H. B., and Winkler, J. R. (2007) *J. Phys. Chem. B* **111**, 2107–2112
58. Bertoncini, C. W., Fernandez, C. O., Griesinger, C., Jovin, T. M., and Zweckstetter, M. (2005) *J. Biol. Chem.* **280**, 30649–30652
59. Rospigliosi, C. C., McClendon, S., Schmid, A. W., Ramlall, T. F., Barré, P., Lashuel, H. A., and Eliezer, D. (2009) *J. Mol. Biol.* **388**, 1022–1032
60. Drescher, M., Veldhuis, G., van Rooijen, B. D., Milikisyants, S., Subramaniam, V., and Huber, M. (2008) *J. Am. Chem. Soc.* **130**, 7796–7797
61. Bortolus, M., Tombolato, F., Tessari, I., Bisaglia, M., Mammi, S., Bubacco, L., Ferrarini, A., and Maniero, A. L. (2008) *J. Am. Chem. Soc.* **130**, 6690–6691
62. Eliezer, D. (2008) in *Parkinson's Disease: Molecular and Therapeutic Insights from Model Systems* (Nass, R., and Przedborski, S., eds) pp. 575–595, Academic Press, New York
63. Ramakrishnan, M., Jensen, P. H., and Marsh, D. (2003) *Biochemistry* **42**, 12919–12926
64. Kamp, F., and Beyer, K. (2006) *J. Biol. Chem.* **281**, 9251–9259
65. Madine, J., Doig, A. J., and Middleton, D. A. (2006) *Biochemistry* **45**, 5783–5792
66. Pandey, A. P., Haque, F., Rochet, J. C., and Hovis, J. S. (2009) *Biophys. J.* **96**, 540–551
67. Madine, J., Hughes, E., Doig, A. J., and Middleton, D. A. (2008) *Mol. Membr. Biol.* **25**, 518–527
68. Bodner, C. R., Dobson, C. M., and Bax, A. (2009) *J. Mol. Biol.* **390**, 775–790
69. Abeliovich, A., Schmitz, Y., Fariñas, I., Choi-Lundberg, D., Ho, W. H., Castillo, P. E., Shinsky, N., Verdugo, J. M., Armanini, M., Ryan, A., Hynes, M., Phillips, H., Sulzer, D., and Rosenthal, A. (2000) *Neuron* **25**, 239–252
70. Larsen, K. E., Schmitz, Y., Troyer, M. D., Mosharov, E., Dietrich, P., Quazi, A. Z., Savalle, M., Nemani, V., Chaudhry, F. A., Edwards, R. H., Stefanis, L., and Sulzer, D. (2006) *J. Neurosci.* **26**, 11915–11922
71. Chandra, S., Fornai, F., Kwon, H. B., Yazdani, U., Atasoy, D., Liu, X., Hammer, R. E., Battaglia, G., German, D. C., Castillo, P. E., and Südhof, T. C. (2004) *Proc. Natl. Acad. Sci. U.S.A.* **101**, 14966–14971
72. Chandra, S., Gallardo, G., Fernández-Chacón, R., Schlüter, O. M., and Südhof, T. C. (2005) *Cell* **123**, 383–396

Helix Interconversion of α -Synuclein

73. Cooper, A. A., Gitler, A. D., Cashikar, A., Haynes, C. M., Hill, K. J., Bhullar, B., Liu, K., Xu, K., Strathearn, K. E., Liu, F., Cao, S., Caldwell, K. A., Caldwell, G. A., Marsischky, G., Kolodner, R. D., Labaer, J., Rochet, J. C., Bonini, N. M., and Lindquist, S. (2006) *Science* **313**, 324–328
74. Ferreon, A. C., Moran, C. R., Ferreon, J. C., and Deniz, A. A. (2010) *Angewandte Chemie* **49**, 3469–3472
75. Rhoades, E., Ramlall, T. F., Webb, W. W., and Eliezer, D. (2006) *Biophys. J.* **90**, 4692–4700
76. Ulmer, T. S., and Bax, A. (2005) *J. Biol. Chem.* **280**, 43179–43187
77. Fredenburg, R. A., Rospigliosi, C., Meray, R. K., Kessler, J. C., Lashuel, H. A., Eliezer, D., and Lansbury, P. T., Jr. (2007) *Biochemistry* **46**, 7107–7118